FGF-1 reverts epithelial-mesenchymal transition induced by TGF- β1 through MAPK/ERK kinase pathway

Carlos Ramos, Carina Becerril, Martha Montaño, Carolina García-De-Alba, Remedios Ramírez, Marco Checa, Annie Pardo and Moisés Selman

Am J Physiol Lung Cell Mol Physiol 299:L222-L231, 2010. First published 21 May 2010; doi:10.1152/ajplung.00070.2010

Am J Physiol Lung Cell Mol Physiol 299: L222–L231, 2010.
First published May 21, 2010; doi:10.1152/ajplung.00070.2010.

FGF-1 reverts epithelial-mesenchymal transition induced by TGF-β1 through MAPK/ERK kinase pathway

Carlos Ramos,[1] Carina Becerril,[1] Martha Montaño,[1] Carolina García-De-Alba,[1] Remedios Ramírez,[2] Marco Checa,[1] Annie Pardo,[2] and Moisés Selman[1]

[1]*Instituto Nacional de Enfermedades Respiratorias Ismael Cosío Villegas and* [2]*Facultad de Ciencias, Universidad Nacional Autónoma de México, México City, México*

Submitted 1 March 2010; accepted in final form 20 May 2010

Ramos C, Becerril C, Montaño M, García-De-Alba C, Ramírez R, Checa M, Pardo A, Selman M. FGF-1 reverts epithelial-mesenchymal transition induced by TGF-β1 through MAPK/ERK kinase pathway. *Am J Physiol Lung Cell Mol Physiol* 299: L222–L231, 2010. First published May 21, 2010; doi:10.1152/ajplung.00070.2010.—Idiopathic pulmonary fibrosis (IPF) is a progressive and lethal lung disease characterized by the expansion of the fibroblast/myofibroblast population and aberrant remodeling. However, the origin of mesenchymal cells in this disorder is still under debate. Recent evidence indicates that epithelial-mesenchymal transition (EMT) induced primarily by TGF-β1 plays an important role; however, studies regarding the opposite process, mesenchymal-epithelial transition, are scanty. We have previously shown that fibroblast growth factor-1 (FGF-1) inhibits several profibrogenic effects of TGF-β1. In this study, we examined the effects of FGF-1 on TGF-β1-induced EMT. A549 and RLE-6TN (human and rat) alveolar epithelial-like cell lines were stimulated with TGF-β1 for 72 h, and then, in the presence of TGF-β1, were cultured with FGF-1 plus heparin for an additional 48 h. After TGF-β1 treatment, epithelial cells acquired a spindle-like mesenchymal phenotype with a substantial reduction of E-cadherin and cytokeratins and concurrent induction of α-smooth muscle actin measured by real-time PCR, Western blotting, and immunocytochemistry. FGF-1 plus heparin reversed these morphological changes and returned the epithelial and mesenchymal markers to control levels. Signaling pathways analyzed by selective pharmacological inhibitors showed that TGF-β1 induces EMT through Smad pathway, while reversion by FGF-1 occurs through MAPK/ERK kinase pathway, resulting in ERK-1 phosphorylation and Smad2 dephosphorylation. These findings indicate that TGF-β1-induced EMT is reversed by FGF-1 and suggest therapeutic approaches to target this process in IPF.

pulmonary fibrosis; mesenchymal-epithelial transition; Smad2

IDIOPATHIC PULMONARY FIBROSIS (IPF) is a progressive, irreversible, and lethal lung disease characterized by epithelial cell injury and activation, expansion of the fibroblast/myofibroblast population, and extracellular matrix remodeling, resulting in an irreversible distortion of the lung architecture (17, 31). Mesenchymal cells accumulate in discrete small collections of spindle-shaped fibroblasts and myofibroblasts within myxoid stroma forming the so-called fibroblastic foci (15). These foci are considered to represent areas of active disease. Myofibroblasts, the α-smooth muscle actin (α-SMA)-expressing fibroblasts, are shown to be the main source of type I collagen and fibrogenic cytokines in fibrotic lesions, and also contribute to the altered mechanical properties of affected lungs (27).

The origin of fibroblasts in these fibroblastic foci has not been definitely elucidated. Migration and proliferation of resident mesenchymal cells and recruitment of fibrocytes may account for a fraction of them; however, emerging evidence indicates that an important number of matrix-producing fibroblasts/myofibroblasts may arise through a mechanism of epithelial-mesenchymal transition (EMT) (2, 16, 20, 27, 31, 32, 41).

EMT and its opposite, mesenchymal-epithelial transition (MET), are crucial for germ layer formation and cell migration in the early vertebrate embryo (1). Thus, EMT processes are essential for the progress of embryonic development, and, although usually maintained in a silent state in the adult, it may transiently turn-on for wound healing and tissue repair (1, 13). However, the abnormal activation of EMT programs has been associated with tissue fibrosis, cancer invasion, and metastasis (1, 9, 13, 16, 20, 25, 34, 38, 41, 45).

EMT involves a functional transition of polarized epithelial cells into migratory mesenchymal cells. During this process, cells lose many of their epithelial hallmarks such as strong inter-cell adhesion and polarity, show decreased expression of epithelial markers such as E-cadherin and acquire a mesenchymal phenotype including spindle-shaped morphology switching expression from keratin- to vimentin-type intermediate filaments, and become isolated, motile, and resistant to anoikis (18).

TGF-β1, a potent profibrotic factor, plays a pivotal role promoting EMT in normal development and in pathological processes, including the alveolar epithelial cell transition to myofibroblasts in vitro and in vivo (1, 16, 20, 41, 42, 44). More recently, a number of mediators able to induce EMT, such as WNT1-inducible signaling protein-1 (WISP1) and endothelin-1, have also been described (10, 19). However, studies regarding the converse process MET are scanty. Recently, it was shown that hepatocyte growth factor induces the upregulation of Smad7 and prevents acquisition of a myofibroblast phenotype in lung epithelial cells stimulated with TGF-β, thereby potentially reversing EMT (35).

We have previously demonstrated that acidic fibroblast growth factor-1 (FGF-1) displays antifibrotic functions downregulating collagen expression and antagonizing some profibrotic effects of TGF-β (4, 29).

In this study, we present evidence that FGF-1 reverts TGF-β1-induced EMT in alveolar epithelial-like cells throughout MEK-ERK pathway inducing the dephosphorylation of Smad2.

Address for reprint requests and other correspondence: M. Selman, Instituto Nacional de Enfermedades Respiratorias, Tlalpan 4502, CP 14080, México City, México (e-mail: moiselman@salud.gob.mx; mselmanl@yahoo.com.mx).

MATERIALS AND METHODS

Epithelial to mesenchymal transition. A549 human lung epithelial-like cells and RLE-6TN, rat alveolar epithelial-like cells, were obtained from American Type Culture Collection. Human cells were cultured in Ham's F-12 and rat cells in Ham's F-12 and DMEM (vol/vol) containing 10% FBS, 100 U/ml penicillin, 100 μg/ml streptomycin, and 2.5 μg/ml amphotericin B at 37°C in a humidified atmosphere of 5%–95% CO_2-ambient air. Experiments were performed when A549 and RLE-6TN epithelial cells reached 50% and 30% confluence, respectively. To induce EMT, cells were stimulated for 72 h in serum-free medium (SFM) with 0.1% BSA and TGF-β1 (5 ng/ml); then, to evaluate the effect of FGF-1, the culture medium was replaced with SFM supplemented with 0.1% BSA, TGF-β1 (5 ng/ml), and recombinant human FGF-1 (R&D, Minneapolis, MN; 20 ng/ml) plus heparin (100 μg/ml) or TGF-β1 alone, and cells were incubated for 48 additional hours. Control cells were maintained in SFM with 0.1% BSA for 120 h. Conditioned media (CM) were collected and frozen at −70°C until use. Cells were used for immunocytochemistry, RT-PCR, and Western blot.

Immunofluorescence and confocal microscopy. A549 cells (1×10^4 cells/cm^2) grown on cover slips and treated as specified above were fixed for 3 min with methanol at room temperature, followed by acetone at −20°C for 2 min; then they were washed and kept in PBS at 4°C. Nonspecific binding was blocked with 10% goat serum in PBS-Tween 20 0.5%. Cells were incubated with FITC-conjugated anti-α-SMA (1:100 dilution; Sigma, St. Louis, MO) and mouse MAb for human E-cadherin (1:25 dilution; Santa Cruz Biotechnology, Santa Cruz, CA) overnight at 4°C and then washed with PBS-Tween 0.5% and incubated with Alexa 633-conjugated goat anti-mouse antibody (5 μg/ml; Molecular Probes, Invitrogen) for 1 h at room temperature. At the end, the preparations were treated with mounting medium containing DAPI to stain cell nuclei (Ultra Cruz Mounting Medium, Santa Cruz Biotechnology). For fluorescence analyses, a confocal laser scanning microscope (Leica TCS SP5; Wetzlar, Germany) was used. Sequential scanning for the different fluorophores was performed, and the images were then merged.

Signaling pathways analysis. A549 cells were incubated for 72 h with TGF-β1, preincubated 1 h with specific inhibitors, and subsequently incubated for an additional 48 h with TGF-β1 plus FGF-1/H. Inhibitors included PD-098059 [MAPK ERK kinase (MEK) inhibitor, 40 μM; Calbiochem, San Diego, CA], LY-294002 (phosphatidylinositol 3-kinase, 50 μM; Cell Signaling Technology, Beverly, MA), SB-203580 (p38-MAPK pathway, 20 μM; Calbiochem), and SB-431542 (TGF-β1 type I receptor kinase, 10 μM; Calbiochem). Signaling pathways were examined by immunoblotting.

Western blotting. Cells were lysed in RIPA buffer M-PER (Pierce, Cheshire, UK) containing a protease inhibitor cocktail (P8340; Sigma). Protein concentrations were determined by Bradford method. Equal amounts of proteins (40 μg) were resolved in 10% SDS-PAGE and transferred onto a Hybond ECL membrane (Amersham, Buckinghamshire, UK). After blocking with non-fat dried milk, the membranes were incubated with primary mouse monoclonal antibodies for 1 h at room temperature followed by detection using horseradish peroxidase-labeled anti-mouse antibody. Primary antibodies included anti-human E-cadherin (Biogenex Lab, San Ramon, CA; 2:1,000 dilution), α-SMA (Sigma; 1:300), Smad2 (Santa Cruz Biotechnology; 1:1,000), phospho-Smad2 (Santa Cruz Biotechnology; 1:100), Erk1/2 (Santa Cruz Biotechnology; 2:1,000), phosphorylated Erk1/2 (5:1,000 dilution; Santa Cruz Biotechnology), and β-tubulin (1:200 dilution; Santa Cruz Biotechnology). Also, anti-rat E-cadherin (Biogenex Lab; 2:1,000 dilution) and α-SMA (Sigma-Aldrich, St. Louis, MO; 1:300 dilution) were used. The proteins were revealed by an enhanced chemiluminescence detection system (Amersham Biosciences). Band densities were digitalized and quantified using image analysis software (ID; Eastman Kodak, Rochester, NY). Results were expressed as a ratio of band density to total β-tubulin. Changes in levels of phosphorylated proteins were assessed with reference to the respective non-phosphorylated proteins.

Gelatin zymography. Zymography was used to identify proteins with gelatinolytic activity in CM as described elsewhere (26). Briefly, samples were mixed with an equal volume of 2× sample buffer, resolved under nonreducing conditions on 7.5% SDS-PAGE containing 1 mg/ml gelatin as a substrate. CM from human lung fibroblasts and from U2-OS cells stimulated with PMA was used as MMP-2 and MMP-9 positive controls, respectively. Band densities were digitalized and quantified using image analysis software (ID).

Real-time quantitative RT-PCR. Total RNA was extracted from epithelial cells using TRIzol reagent (Invitrogen Life Technologies, Grand Island, NY) and reversed transcribed into cDNA (Advantage RT-for-PCR Kit; Clontech, Palo Alto, CA) according to the manufacturer's instructions. RT-PCR amplification was performed with the i-Cycler iQ Detection System (BioRad, Hercules, CA) using TAQMAN

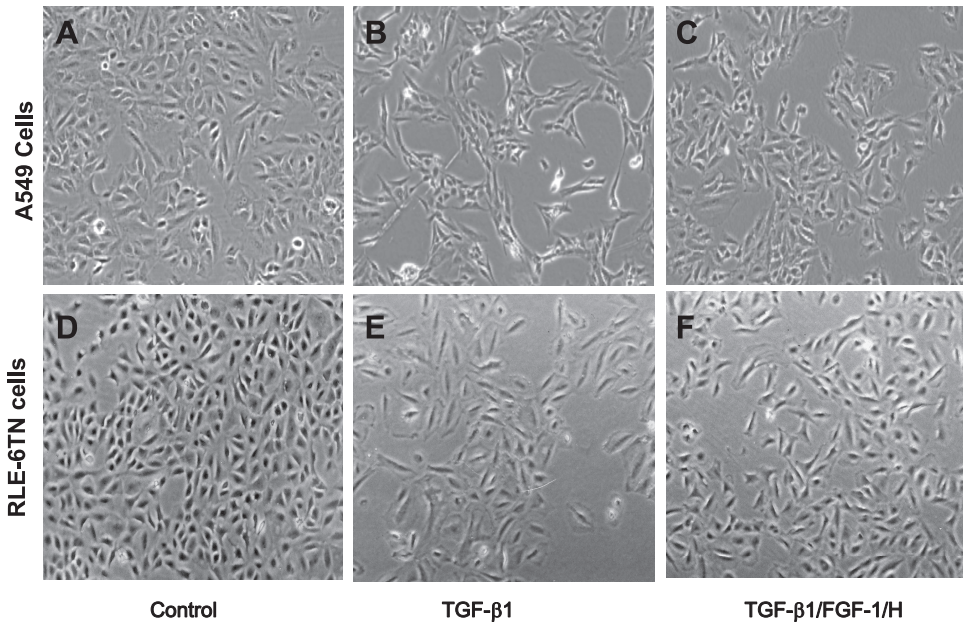

Fig. 1. FGF-1/H reverts TGF-β1-induced changes in epithelial morphology. Human (A549) and rat (RLE-6TN) epithelial cells cultured in the absence of TGF-β1 maintain the typical polygonal/cobblestone or round appearance (*A* and *D*). After stimulation with TGF-β1 for 72 h, the epithelial cells assumed an elongated, spindle-shape, fibroblast-like morphology (*B* and *E*). FGF-1 plus heparin reverts changes induced by TGF-β1 and restores cells to their epithelial morphology (*C* and *F*). Original magnification, ×10.

probes (PE Applied Biosystems, Wellesley, CA) labeled with FAM for E-cadherin (Hs 01023895_M1), α-SMA (Hs 00909449_M1), and 18S rRNA (4352930E) as endogenous control. PCR was performed with the cDNA working mixture in a 25-μl reaction volume containing 3 μl of cDNA, 2 mM $MgCl_2$, 0.2 mM dNTPs, 0.2 μM of each TAQMAN probe and 2.5 units of recombinant Taq DNA polymerase (Invitrogen). A dynamical range was built with each product of PCR on copy number serial dilutions from 1×10^8 to 1×10^1. Standard curves were calculated referring the threshold cycle (Ct) to the log of each cDNA. Results were expressed as the number of copies of the target gene normalized to 18S rRNA. The PCR conditions were 2 min at 94°C followed by 40 cycles of 15 s at 94°C and 1 min at 60°C.

Apoptosis of epithelial cells. A549 cells were grown to 70% confluence in T-25 culture flasks. Apoptosis was determined by annexin-V staining assessed by flow cytometry in cells stimulated with recombinant human FGF-1 (20 ng/ml) and controls, as follows: harvested cells were incubated with Annexin V-PE and 7AAD (BD Bioscience, San Diego, CA) following the manufacturer's instructions. Apoptotic cell death (Annexin-V+, 7AAD-) was measured by flow cytometry using a FACSAria cytometer. The results were analyzed with Flow Jo software. Two independent experiments were performed by duplicate.

Immunohistochemistry. Tissue sections from IPF and controls were treated as previously described (33). Antigen retrieval was performed in citrate buffer (10 mM, pH 6.0) for 6 min in a microwave. Samples were incubated with anti-human anti-FGF-1 mouse monoclonal (Abcam, Cambridge, MA; 3 μg/ml) at 4°C overnight. A secondary biotinylated anti-immunoglobulin followed by horseradish peroxidase-conjugated streptavidin (BioGenex, San Ramon, CA) was used according to the manufacturer's instructions. 3-Amino-9-ethyl-carbazole (AEC; BioGenex) in acetate buffer containing 0.05% H_2O_2 was used as substrate. The sections were counterstained with hematoxylin. The primary antibody was replaced by nonimmune serum for negative control slides.

Statistical analysis. Results are presented as means ± SD of at least three independent experiments. Statistical analysis was performed with ANOVA followed by Dunnett's multiple comparison post hoc tests. $P < 0.05$ was considered statistically significant.

RESULTS

TGF-β1-induced EMT is reversed by FGF-1/H. After TGF-β1 treatment, A549 human lung epithelial-like cells lost cell-cell contact and turned into a spindle-like mesenchymal phenotype (Fig. 1). A549 cell line treated with FGF-1/H in the presence of TGF-β1 recovered their polygonal/cobblestone phenotype. Similar results were obtained with rat alveolar epithelial-like cells RLE-6TN (Fig. 1). This morphological change was accompanied by a substantial reduction, demonstrated at the gene and protein level, of the characteristic epithelial phenotypic marker E-cadherin (Fig. 2, *A* and *B*) with

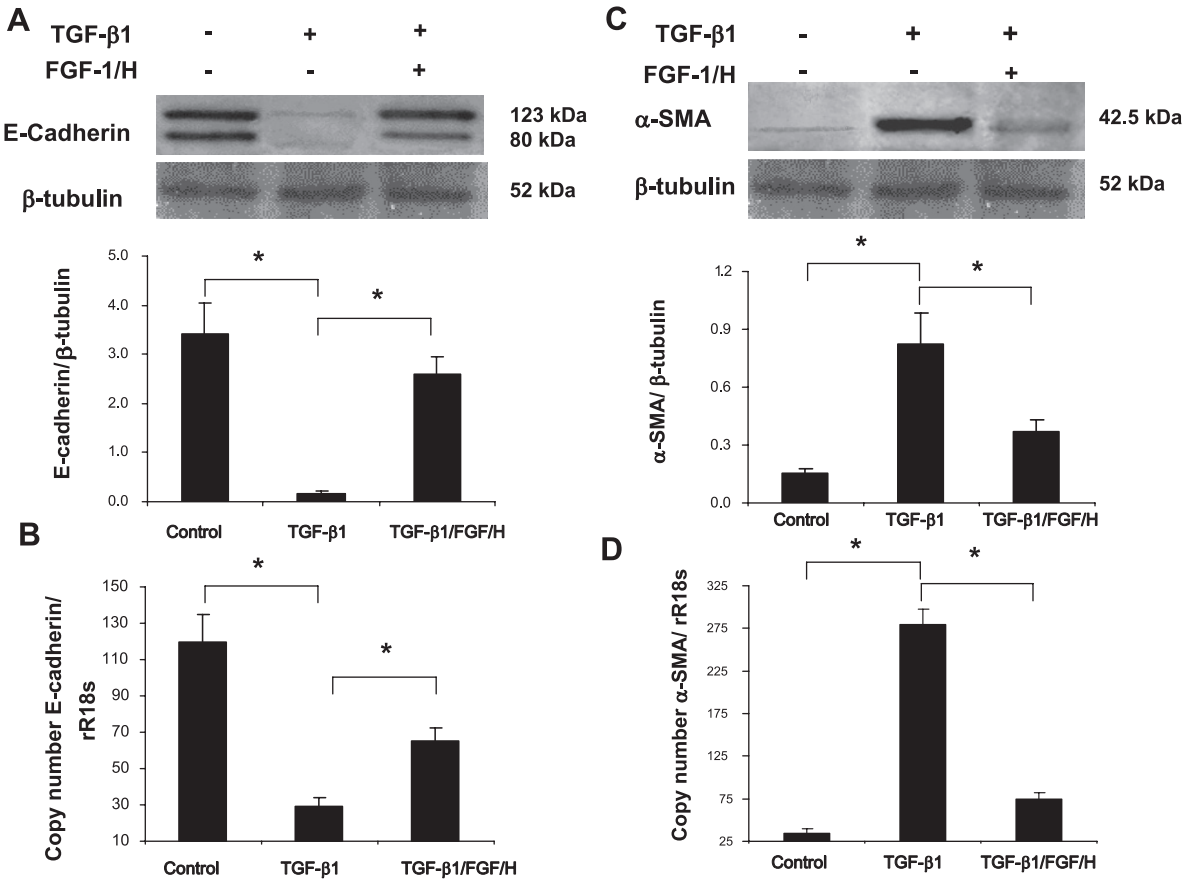

Fig. 2. Effect of FGF-1/H on the expression of E-cadherin and α-smooth muscle actin (α-SMA) in TGF-β1-induced epithelial-mesenchymal transition (EMT) in A549 epithelial cells. Cells were stimulated with TGF-β1 for 72 h and then with FGF-1/H plus TGF-β1 or TGF-β1 alone during 48 h. *A*: E-cadherin protein expression was downregulated ~6-fold compared with untreated cells. FGF-1/H restored the expression almost to control levels as demonstrated by densitometry analysis. *B*: real-time quantitative RT-PCR for E-cadherin showed similar results. *C*: TGF-β1 strongly increased the expression of α-SMA protein compared with untreated cells. FGF-1/H inhibited this effect restoring expression close to control levels. *D*: real-time quantitative RT-PCR for α-SMA revealed similar results. Each bar represents means ± SD of 3 independent experiments; $*P < 0.01$.

concurrent and significant induction of the mesenchymal marker α-SMA (Fig. 2, *C* and *D*), and also of vimentin (not shown). After treatment with FGF1/H, the expression of both E-cadherin and α-SMA returned to control levels as demonstrated by Western blot and real-time RT-PCR (Fig. 2). Comparable results for E-cadherin expression was obtained when rat RLE-6TN cells were treated with FGF-1/H (Fig. 3*A*). Also, α-SMA that is usually expressed by these cells (22) was upregulated by TGF-β1 and returned to basal levels after treatment with FGF-1H (Fig. 3*B*). Treatment of epithelial cells with heparin alone showed no effect (not shown).

Confocal immunofluorescence microscopy using double-labeling for E-cadherin (red) and α-SMA (green) corroborated these results. As shown in Fig. 4, control A549 epithelial cells displayed intense E-cadherin labeling without α-SMA expression. Incubation of A549 cells with TGF-β1 strongly reduced E-cadherin immunostaining while an intense α-SMA expression was observed. When epithelial cells were incubated with TGF-β1 for 72 h followed by an additional 48 h with FGF-1/H, labeling for both E-cadherin and α-SMA regressed to control levels. Since we have previously demonstrated that FGF-1 induces cell death in mesenchymal cells (29), we evaluated this effect on A549 epithelial-like cells. Our results showed that FGF-1 did not induce apoptosis on this cell line (1.49 ± 0.26 in controls vs. 1.61 ± 0.33 in FGF-1-stimulated cells).

FGF1 reverts the increase of MMP-2 and MMP-9 induced by TGF-β1. It is known that during TGF-β1-induced EMT, alveolar and other epithelial cells increase the expression of gelatinases, mainly MMP-2, that are necessary to acquire the cell migratory phenotype characteristic of mesenchymal cells (14, 21). As illustrated in the zymogram of Fig. 5, under basal conditions A549 cells show moderate activity bands of gelatinases MMP-2 and MMP-9. After TGF-β1 treatment, there is a strong increase of both MMP-2 and MMP-9 enzymes. When cells were incubated with TGF-β1 and then with FGF-1/H, MMP-2 and MMP-9 activities returned to control levels.

FGF-1 reverts TGF-β1-induced EMT through MEK-dependent signaling. To analyze the signaling pathways involved in EMT reversion induced by FGF-1, we used several pharmacological inhibitors. A549 cells were incubated for 72 h with TGF-β1 and then preincubated 1 h with specific inhibitors and subsequently incubated for additional 48 h with TGF-β1 plus FGF-1/H and inhibitors. As previously demonstrated, downregulation of E-cadherin by TGF-β1 (Fig. 6) is reverted by FGF-1/H. When the effects of different pharmacological inhibitors were compared with the band intensity of FGF-1/H, the MEK inhibitor PD-098059 was the only one blocking significantly the reversion of E-cadherin suggesting that this pathway is implicated in the effect of FGF-1 on EMT. A modest effect was also observed when p38 and PI3K were antagonized, whereas inhibition of TGF-β1 type I receptor kinase showed no effect. We also used the TGF-β1 type I receptor kinase inhibitor in absence of FGF-1 observing that this inhibitor successfully abolished the effect of TGF-β1 on E-cadherin expression (Fig. 6).

The role of MEK kinase signaling pathway in the FGF-1-induced EMT reversion was further corroborated. As shown in Fig. 7, PD-098059 (MEK inhibitor) abolished the effect of FGF-1/H on E-cadherin. The inhibitor alone had no effect. Also, the inhibitor did not affect the reduction of E-cadherin expression induced by TGF-β1 indicating that MEK/ERK pathway is not involved in TGF-β1-induced EMT. Additionally, we demonstrated that FGF1/H phosphorylates Erk-1 (Fig. 8*A*).

FGF-1 inhibits Smad2 phosphorylation. Although the molecular mechanisms governing TGF-β1-induced EMT remain unclear, most evidence indicates that it may be mainly regu-

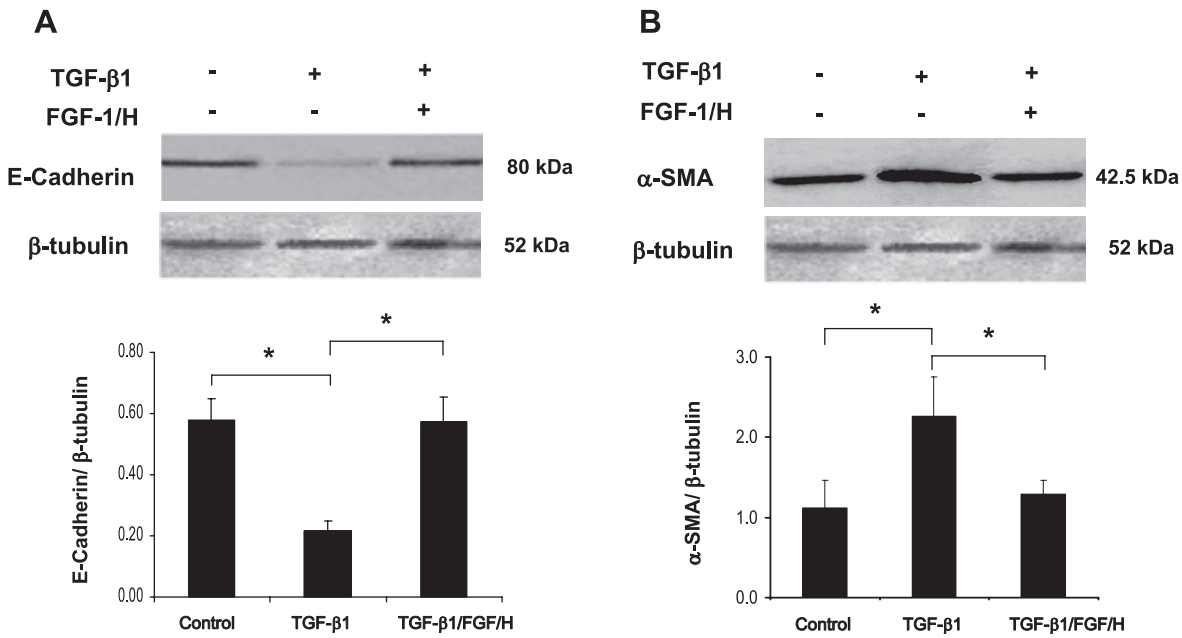

Fig. 3. Expression of epithelial and mesenchymal markers in response to TGF-β1 and FGF-1/H in RLE-6TN epithelial cells. Cells were incubated in the presence of TGF-β1 for 72 h, and then with FGF-1 plus heparin or TGF-β1 alone during 48 h. *A*: E-cadherin protein expression was downregulated ~3-fold compared with untreated cells. FGF-1/H returned the expression to control levels. *B*: α-SMA was overexpressed after TGF-β1 stimulation, and the levels returned to basal after treatment with FGF-1/H. Each bar represents means ± SD of 2 independent experiments; $*P < 0.01$.

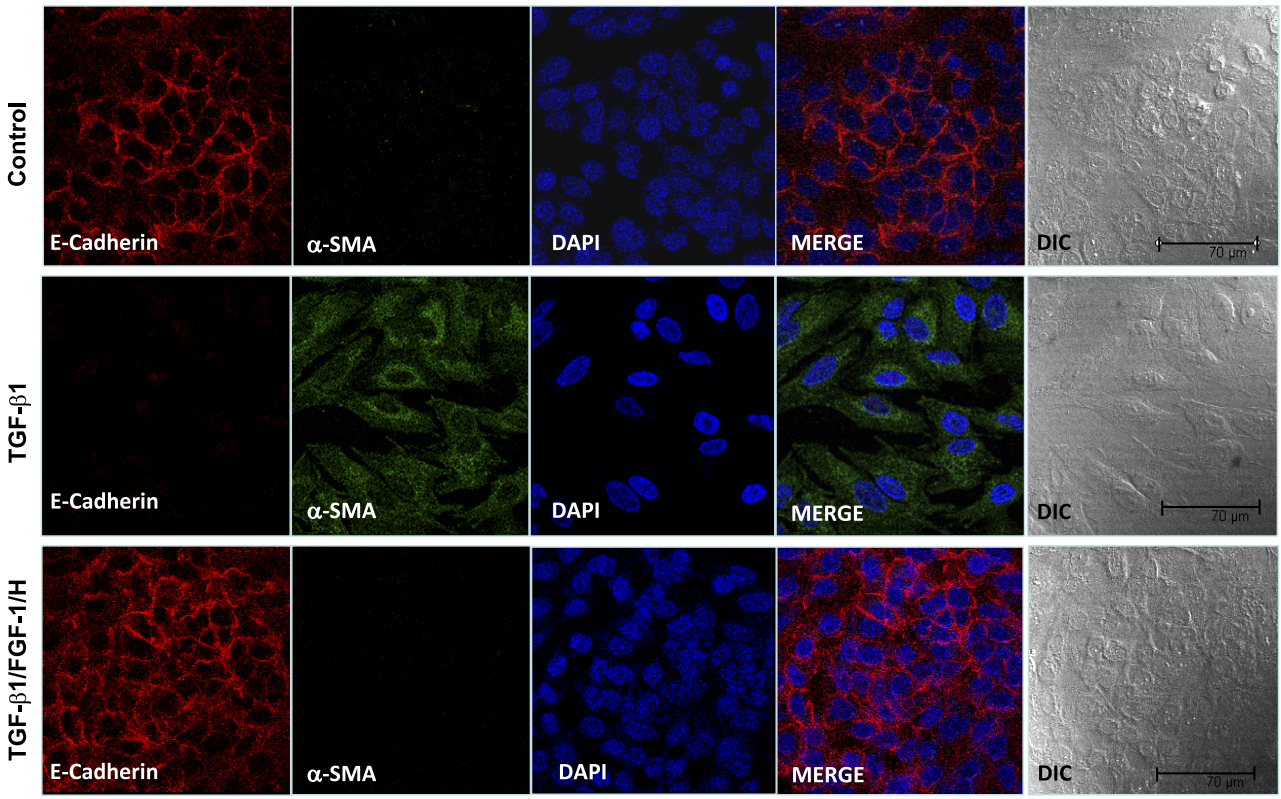

Fig. 4. FGF-1/H reverts TGF-β1-induced EMT as detected by confocal immunofluorescence microscopy. A549 epithelial cells were grown on coverslips and treated with TGF-β1 for 72 h and then with TGF-β1 and FGF-1/H or TGF-β1 alone for 48 additional h. Cells were fixed and stained with α-SMA and E-cadherin antibodies followed by incubation with fluorescent dye-tagged secondary antibodies. DAPI was used to stain nuclei. α-SMA (green), E-cadherin (red), and nuclei (blue) were visualized by confocal fluorescence microscopy (original magnification, ×40). Differential interference contrast (DIC) is included in the last column. Following treatment with TGF-β1, E-cadherin immunoreactivity was substantially diminished while α-SMA was strongly expressed, indicating the cells were undergoing EMT. FGF-1 plus heparin markedly attenuated this effect.

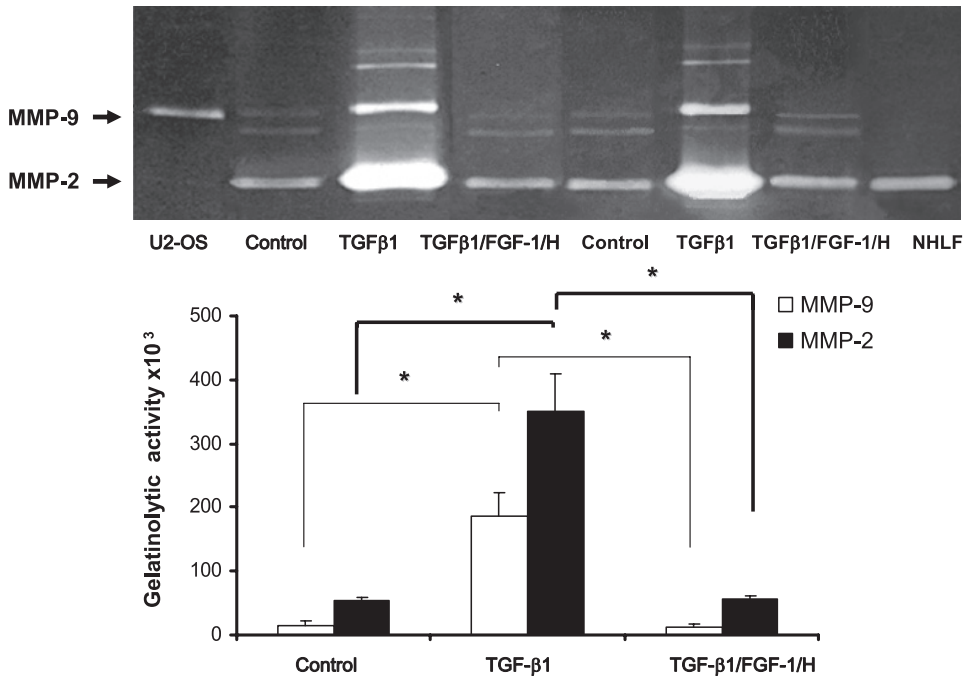

Fig. 5. Effect of TGF-β1 and TGF-β1 plus FGF-1/H on MMP-2 and MMP-9 activities. Conditioned medium from untreated A549 cells and from TGF-β1- or TGF-β1 plus FGF-1/H-treated cells was subjected to the analysis of gelatinolytic activities by zymography in 2 independent experiments. Shown are U2-OS cells as marker of pro-MMP-9 and human lung fibroblasts (NHLF) as marker for pro-MMP-2. TGF-β1 caused a strong increase of MMP-2 and MMP-9 band activities, which was regressed by FGF-1/H. The image represents the densitometric quantitative analysis of the surface and intensity of the gelatinolytic bands displayed (*top*). $^*P < 0.01$.

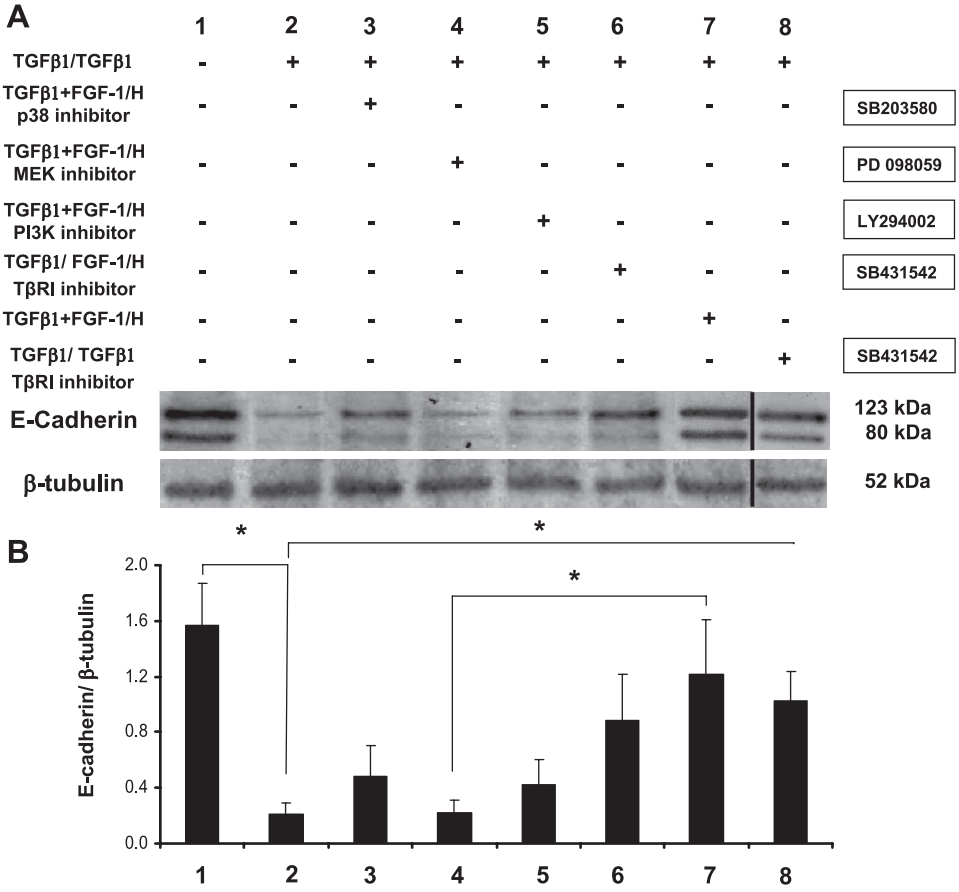

Fig. 6. FGF-1/H reverts TGF-β1-induced E-cadherin downregulation mainly through MEK/ERK kinase pathway. Cells were cultured in serum-free medium containing TGF-β1 for 72 h, then preincubated for 1 h with specific inhibitors and subsequently incubated for additional 48 h with TGF-β1/FGF-1/H or TGF-β1 alone. Cells were lysed, electrophoresed, transferred onto nitrocellulose membranes, and immunoblotted as described in MATERIALS AND METHODS. *A*: *Lane 1*: A549 control cells. *Lanes 2* and *8*: A549 cells treated with TGF-β1. *Lanes 3–7*: A549 cells treated with TGF-β1 and FGF-1 plus heparin. *Lane 3*: preincubated with 20 μM SB-203580 (p38-MAPK pathway inhibitor). *Lane 4*: preincubated with 40 μM PD-098059 (MEK/ERK inhibitor). *Lane 5*: preincubated with 50 μM LY-294002 (PI3K inhibitor). *Lanes 6* and *8*: preincubated with 10 μM SB-431542 (inhibitor of the TGF-β1 type I receptor kinase). E-cadherin content was normalized to β-tubulin. Quantitative image analysis showed a significant decrease of E-cadherin bands when MEK/ERK kinase pathway was inhibited (*lane 4*). *B*: each bar represents means ± SD of 3 independent experiments; $*P < 0.01$.

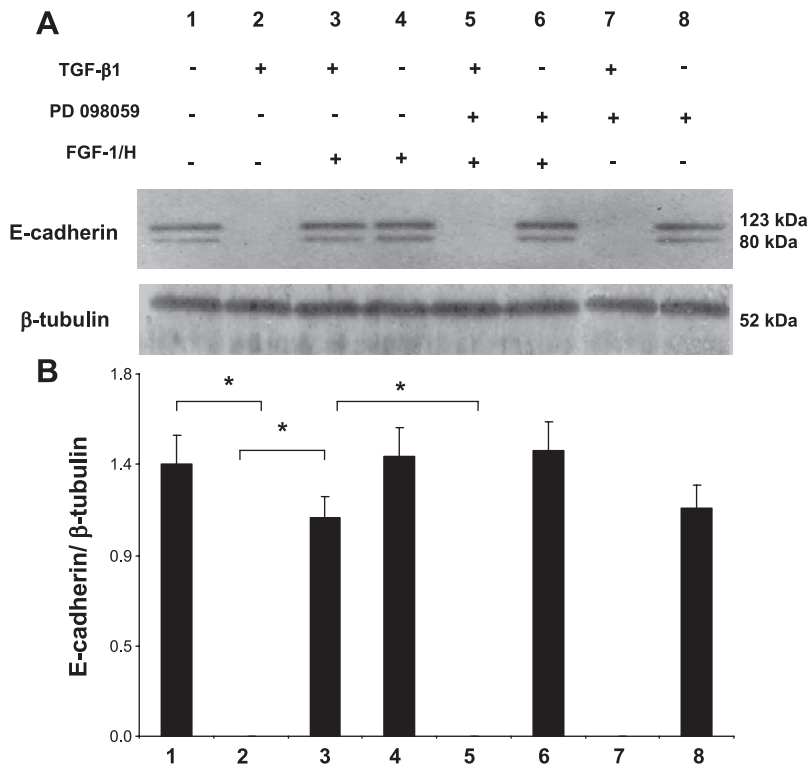

Fig. 7. Effect of the selective inhibition of MEK/ERK pathway on E-cadherin expression. A549 cells were treated with TGF-β1, FGF-1/H, or TGF-β1 plus FGF-1/H, with or without preincubation with 40 μM of specific MEK/ERK inhibitor PD-098059. *A*: *Lane 1*: A549 control cells. *Lane 2*: A549 cells treated with TGF-β1. *Lane 3*: A549 cells treated with TGF-β1 and FGF-1/H. *Lane 4*: A549 cells treated with FGF-1/H. *Lane 5*: A549 cells with TGF-β1, PD-098059, and FGF-1/H. *Lane 6*: A549 cells preincubated with PD-098059 and incubated with FGF-1/H. *Lane 7*: A549 cells preincubated with PD-098059 and treated with TGF-β1. *Lane 8*: A549 cells treated only with PD-098059. The inhibitor blocked the reexpression of E-cadherin induced by FGF-1 plus heparin. *B*: each bar represents means ± SD of 3 independent experiments; $*P < 0.01$.

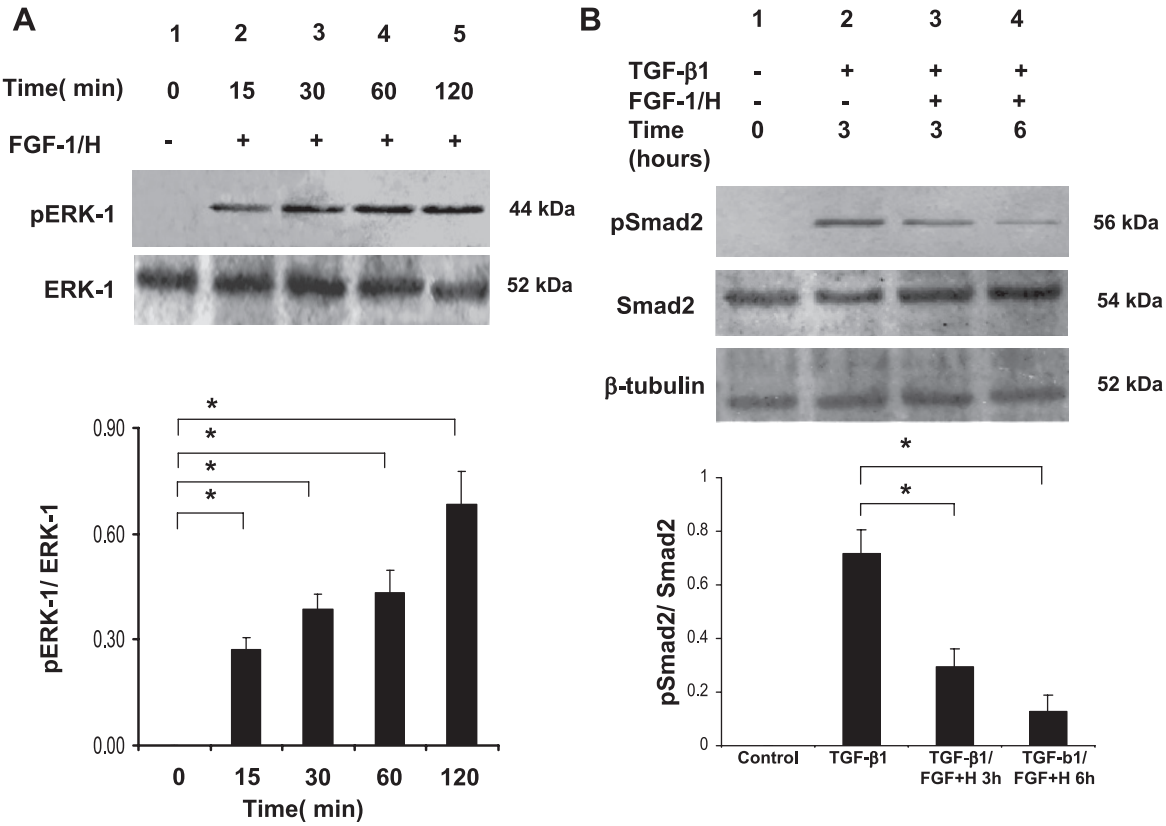

Fig. 8. Effect of FGF-1/H on ERK-1 phosphorylation and TGF-β1-induced Smad2 phosphorylation. A549 epithelial cells treated with FGF-1/H were collected, lysed, electrophoresed, transferred onto nitrocellulose membranes, and immunoblotted for ERK-1 and pERK-1 as described in MATERIALS AND METHODS. *A*: *Lane 1*: A549 control cells. *Lanes 2–5*: A549 cells treated 15, 30, 60, and 120 min with FGF-1 and heparin. *B*: A549 cells were treated for 3 and 6 h with TGF-β1 in presence or absence of FGF-1 plus heparin. *Lane 1*: A549 control cells. *Lane 2*: treatment with TGF-β1 induced phosphorylation of Smad 2. *Lanes 3* and *4*: A549 cells treated with TGF-β1 in presence of FGF-1/H. Quantitative image analysis showed a significant decrement of Smad2 phosphorylation. Each bar represents means ± SD of 3 independent experiments; $*P < 0.01$.

lated by Smads. Therefore, we explored the effect of FGF-1/H on TGF-β1-induced Smad phosphorylation. Epithelial cells were stimulated for 3 and 6 h with TGF-β1 alone or in the presence of FGF-1 plus heparin, and phosphorylation of Smad2 was assessed by Western blot. As shown in Fig. 8*B*, expression of phosphorylated Smad2 protein was increased by TGF-β1. This increase was markedly reduced by the treatment with FGF-1 at 3 and 6 h.

Immunolocalization of FGF-1 in IPF lungs. The localization of FGF-1 was examined by immunohistochemistry in IPF and control lungs. Immunoreactive FGF-1 was found in discrete areas of the IPF lungs. As illustrated in Fig. 9, FGF-1 was localized primarily in the cytoplasm of endothelial cells (Fig. 9*A*) and in some alveolar epithelial-like cells (Fig. 9, *B* and *C*). In addition, FGF-1 was also observed bound to the extracellular matrix. Immunohistochemical staining for FGF-1 was negative in normal lungs as well as in lung tissue samples incubated without the primary antibody.

DISCUSSION

IPF is characterized by epithelial cell injury and activation leading to the formation of fibroblastic foci, the active sites of fibrogenesis (15, 31, 32). Although the origin of fibroblasts in IPF (and other fibrotic lung disorders) is unclear, a growing body of evidence indicates that EMT could be one of them (16, 20, 41). TGF-β1 appears to be the main responsible of this process and may induce the transition of alveolar epithelial-like cells to myofibroblasts, both in vitro and in vivo (16, 41, 44). Wnt/Wingless pathway, that crosstalk with a variety of growth factors including TGF-β, may also play a role in this process. The inhibition of GSK-3, a key component of the Wnt response, leads to the downregulation of E-cadherin and EMT in cultured epithelial cells (3), and recent work indicates that Wnt pathway is upregulated in IPF (19, 34).

Less is known regarding the opposite embryological process MET in adults, although a mesenchymal-to-epithelial reverting transition has been described during metastatic seeding (40). In kidney fibrosis, it has been shown that bone morphogenic protein-7 induces MET in adult renal fibroblasts and facilitates regeneration of injured kidney (47).

In lung fibrosis, it has been recently demonstrated that hepatocyte growth factor induces MET, probably through the upregulation of Smad7, an inhibitor of TGF-β signaling (35).

In the present study, we analyzed the potential role of FGF-1 to revert the TGF-β1-induced EMT. FGF-1 was chosen because previous work in our lab has revealed that it has strong antifibrotic properties and antagonizes TGF-β (4, 29). FGF-1 was used in combination with heparin since it is well known that for the full activation of the FGF receptor by its FGF ligand and subsequent signaling, the presence of heparan sulfate or heparin is required. The mechanism has not been fully elucidated. On one hand, several studies indicate a direct

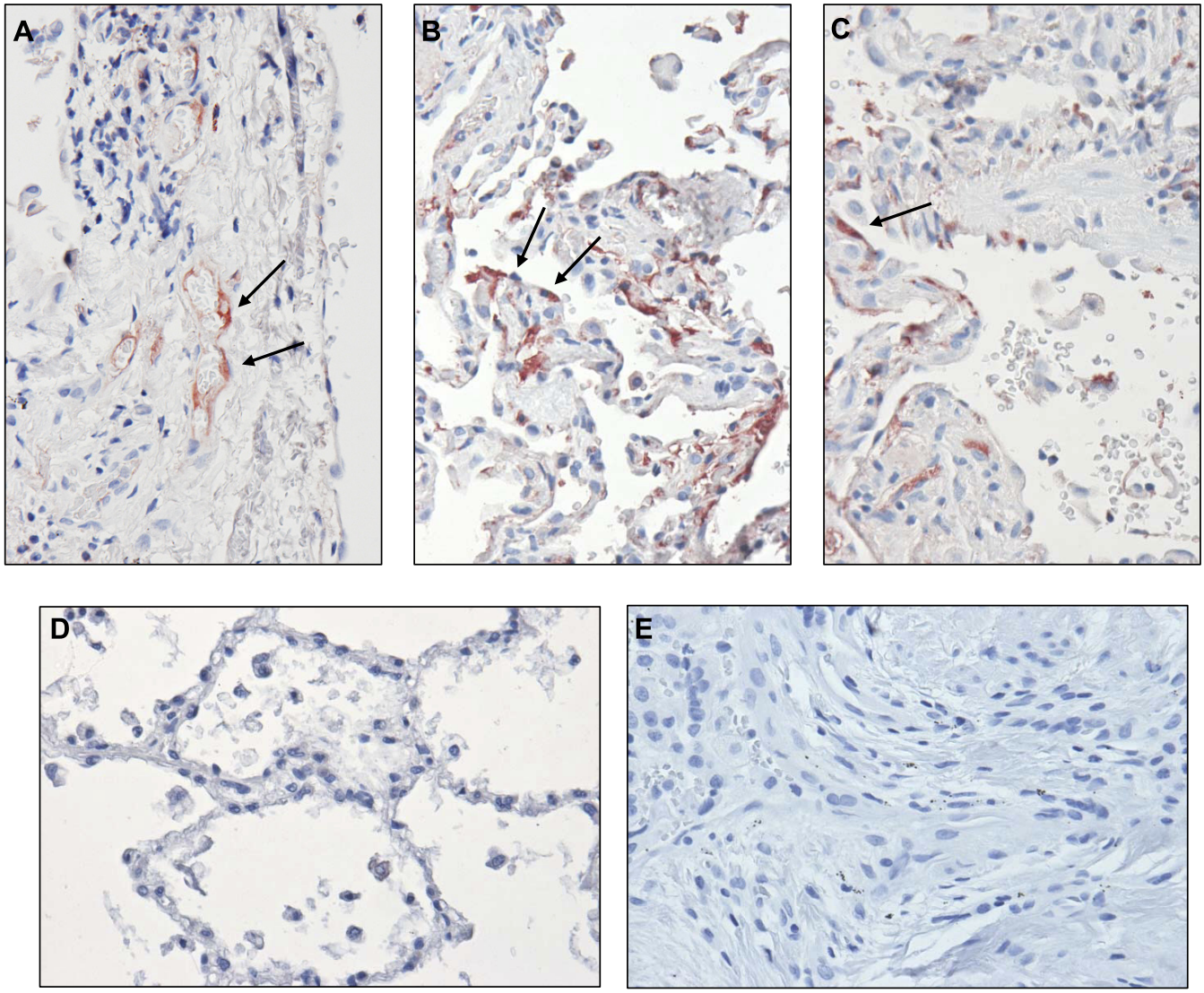

Fig. 9. Immunohistochemical detection of FGF-1 in formalin-fixed, paraffin-embedded IPF and normal lung sections. *A*: endothelial cells from several capillaries are stained for FGF-1 (arrows). *B* and *C*: strong FGF-1 immunostaining in alveolar epithelial cells (arrows) and also bound to extracellular matrix. *D*: normal lungs showed no reactivity. *E*: negative control where the primary antibody was replaced by nonimmune serum.

role for heparin in FGF1-FGFR interaction and receptor activation (30, 48). On the other hand, some recent work suggests that this molecule protects the naturally unstable FGF-1 against heat and/or proteolytic degradation but is not essential for a direct FGF1-FGFR interaction and receptor activation (46).

Our results showed that FGF-1 plus heparin blocked the TGF-β1-induced EMT, reverting the typical phenotype of spindle-like mesenchymal cells to a round/cobblestone epithelial appearance. Accompanying this phenotypic change, we showed that E-cadherin, a key component of adherens junctions and critical in the maintenance of epithelial integrity, was highly reexpressed after FGF-1 stimulation, while the expression of the mesenchymal markers α-SMA and vimentin was strongly downregulated. This effect was observed in two different epithelial cell lines obtained from human and rat lungs. Interestingly, FGF-1 was found in vivo in discrete areas of the IPF lungs and was expressed by elongated alveolar epithelial-like cells and endothelial cells.

The transition to mesenchymal cells induced by TGF-β1 was accompanied by a strong increase of MMP-2 and MMP-9 activities as demonstrated by gelatin zymography, and this effect was also abolished when cells regained the epithelial phenotype induced by FGF-1. It has been described that the transition from epithelial to a mesenchymal phenotype, both in fibrosis and cancer, results in an upregulation of MMP-2, a matrix-degrading enzyme (14, 28, 36). Increased activity of MMP-2 augments the migratory capacity of fibroblasts and enhances invasion and metastasis by cancer cells. Also, the developmentally regulated expression of MMP-2 correlates with the EMT that generates the neural crest, the sclerotome, and dermatome, suggesting that this enzyme is critically involved in the transformation of epithelia to mesenchyme, and also in the later dispersion of mesenchymal tissues (6). Upregulation of MMP-9 has also been described in some models of EMT (5, 8, 37). In a study that evaluated the potential for airway epithelium from lung transplant recipients to undergo

EMT, a threefold increase of MMP-9 was demonstrated with a concomitant increase in the number of invasive cells (5).

The dissection of the signaling mechanisms that are activated in response to TGF-β and lead to EMT has demonstrated a pivotal role of the Smad signaling pathway (42). Increased expression of Smad2 or Smad3 with Smad4 induces EMT, whereas expression of dominant negative versions of Smad2 or Smad3, or the knockdown for Smad4 expression by RNA interference blocks TGF-β-induced EMT (12, 39).

In our study, alveolar epithelial-like cells stimulated with TGF-β1 showed strong phosphorylation of Smad2, which was clearly inhibited by FGF-1 in a time-dependent manner.

To identify the signaling pathway involved in the FGF-1-induced reversion of TGF-β1-elicited EMT, epithelial cells were preincubated with different specific pharmacological inhibitors. Activation of FGFR by FGF-1 allows the recruitment and activation of Src homology (SH2)- or phosphotyrosine (PTB)-containing proteins, leading to the activation of various cytoplasmic signal transduction pathways including PI3K/Akt, MEK1/2-ERK, and p38MAPK (22, 24). Occasionally, in some in vitro systems a dual signaling pathway has been identified. Thus, for example, FGF-1-upregulates MMP-9 expression in ENU1564 cell lines by increasing the activities of NF-κB and AP-1 involving the activation of both PI3K/Akt and MEK1/2-ERK (23).

The results of our study showed that the inhibition of MAPK ERK kinase pathway markedly attenuated the effect of FGF-1 on TGF-β-induced EMT. Thus, when alveolar epithelial-like cells were stimulated with TGF-β1 and then the MEK inhibitor was added the effect of FGF-1, restoring the E-cadherin expression to control levels was inhibited. FGF-1 with heparin alone (without a previous stimulus with TGF-β1) or the MEK inhibitor alone had no effect on E-cadherin expression.

Interestingly, several studies have indicated that ERK signals may repress considerable subsets of intermediate TGF-β target genes and that the MAPK/ERK pathway is also involved in Smad7 upregulation (7, 43).

In summary, this study identifies FGF-1 as an antagonist of TGF-β1-induced EMT inhibiting Smad2 phosphorylation through MEK signaling pathway. This finding suggests that FGF-1 might have a role in the therapy of fibrotic lung disorders where EMT contributes to the expansion of the fibroblast/myofibroblast population. However, additional confirmation with primary human alveolar epithelial cells is necessary.

DISCLOSURES

M. Selman is a consultant of Boehringer Ingelheim.

REFERENCES

1. **Acloque H, Adams MS, Fishwick K, Bronner-Fraser M, Nieto MA.** Epithelial-mesenchymal transitions: the importance of changing cell state in development and disease. *J Clin Invest* 119: 1438–1449, 2009.
2. **Andersson-Sjöland A, de Alba CG, Nihlberg K, Becerril C, Ramírez R, Pardo A, Westergren-Thorsson G, Selman M.** Fibrocytes are a potential source of lung fibroblasts in idiopathic pulmonary fibrosis. *Int J Biochem Cell Biol* 40: 2129–2140, 2008.
3. **Baum B, Settleman J, Quinlan MP.** Transitions between epithelial and mesenchymal states in development and disease. *Semin Cell Dev Biol* 19: 294–308, 2008.
4. **Becerril C, Pardo A, Montaño M, Ramos C, Ramírez R, Selman M.** Acidic fibroblast growth factor induces an antifibrogenic role. *Am J Respir Cell Mol Biol* 20: 1020–1027, 1999.
5. **Borthwick LA, Parker SM, Brougham KA, Johnson GE, Gorowiec MR, Ward C, Lordan JL, Corris PA, Kirby JA, Fisher AJ.** Epithelial to mesenchymal transition (EMT) and airway remodelling after human lung transplantation. *Thorax* 64: 770–777, 2009.
6. **Duong TD, Erickson CA.** MMP-2 plays an essential role in producing epithelial-mesenchymal transformations in the avian embryo. *Dev Dyn* 229: 42–53, 2004.
7. **Dowdy SC, Mariani A, Janknecht R.** Her2/neu- and tak1-mediated up-regulation of the transforming growth factor beta inhibitor smad7 via the ets protein er81. *J Biol Chem* 278: 44377–44384, 2003.
8. **Eastham AM, Spencer H, Soncin F, Ritson S, Merry CL, Stern PL, Ward CM.** Epithelial-mesenchymal transition events during human embryonic stem cell differentiation. *Cancer Res* 67: 11254–11262, 2007.
9. **Iwano M, Plieth D, Danoff TM, Xue C, Okada H, Neilson EG.** Evidence that fibroblasts derive from epithelium during tissue fibrosis. *J Clin Invest* 110: 341–350, 2002.
10. **Jain R, Shaul PW, Borok Z, Willis BC.** Endothelin-1 induces alveolar epithelial-mesenchymal transition through endothelin type A receptor-mediated production of TGF-beta1. *Am J Respir Cell Mol Biol* 37: 38–47, 2007.
11. **Kabashima A, Higuchi H, Takaishi H, Matsuzaki Y, Suzuki S, Izumiya M, Iizuka H, Sakai G, Hozawa S, Azuma T, Hibi T.** Side population of pancreatic cancer cells predominates in TGF-beta-mediated epithelial to mesenchymal transition and invasion. *Int J Cancer* 124: 2771–2779, 2009.
12. **Kaimori A, Potter J, Kaimori JY, Wang C, Mezey E, Koteish A.** Transforming growth factor-1 induces an epithelial-to-mesenchymal transition state in mouse hepatocytes in vitro. *J Biol Chem* 282: 22089–22101, 2007.
13. **Kalluri R, Weinberg RA.** The basics of epithelial-mesenchymal transition. *J Clin Invest* 119: 1420–1428, 2009.
14. **Kasai H, Allen JT, Mason RM, Kamimura T, Zhang Z.** TGF-beta1 induces human alveolar epithelial to mesenchymal cell transition (EMT). *Respir Res* 6: 56, 2005.
15. **Katzenstein AL, Mukhopadhyay S, Myers JL.** Diagnosis of usual interstitial pneumonia and distinction from other fibrosing interstitial lung diseases. *Hum Pathol* 39: 1275–1294, 2008.
16. **Kim KK, Kugler MC, Wolters PJ, Robillard L, Galvez MG, Brumwell AN, Sheppard D, Chapman HA.** Alveolar epithelial cell mesenchymal transition develops in vivo during pulmonary fibrosis and is regulated by the extracellular matrix. *Proc Natl Acad Sci USA* 103: 13180–13185, 2006.
17. **King TE Jr, Schwarz MI, Brown K, Tooze JA, Colby TV, Waldron JA Jr, Flint A, Thurlbeck W, Cherniack RM.** Idiopathic pulmonary fibrosis: relationship between histopathologic features and mortality. *Am J Respir Crit Care Med* 164: 1025–1032, 2001.
18. **Klymkowsky MW, Savagner P.** Epithelial-mesenchymal transition: a cancer researcher's conceptual friend and foe. *Am J Pathol* 174: 1588–1593, 2009.
19. **Königshoff M, Kramer M, Balsara N, Wilhelm J, Amarie OV, Jahn A, Rose F, Fink L, Seeger W, Schaefer L, Günther A, Eickelberg O.** WNT1-inducible signaling protein-1 mediates pulmonary fibrosis in mice and is upregulated in humans with idiopathic pulmonary fibrosis. *J Clin Invest* 119: 772–787, 2009.
20. **Larsson O, Diebold D, Fan D, Peterson M, Nho RS, Bitterman PB, Henke CA.** Fibrotic myofibroblasts manifest genome-wide derangements of translational control. *PLoS One* 3: e3220, 2008.
21. **Li P, Oparil S, Feng W, Chen YF.** Hypoxia-responsive growth factors upregulate periostin and osteopontin expression via distinct signaling pathways in rat pulmonary arterial smooth muscle cells. *J Appl Physiol* 97: 1550–1558, 2004.
22. **Li Y, Yang J, Dai C, Wu C, Liu Y.** Role for integrin-linked kinase in mediating tubular epithelial to mesenchymal transition and renal interstitial fibrogenesis. *J Clin Invest* 112: 503–516, 2003.
23. **Lungu G, Covaleda L, Mendes O, Martini-Stoica H, Stoica G.** FGF-1-induced matrix metalloproteinase-9 expression in breast cancer cells is mediated by increased activities of NF-kappaB and activating protein-1. *Mol Carcinog* 47: 424–435, 2008.
24. **Nishida T, Ito JI, Nagayasu Y, Yokoyama S.** FGF-1-induced reactions for biogenesis of apoE-HDL are mediated by Src in rat astrocytes. *J Biochem* 146: 881–886, 2009.
25. **Omenetti A, Porrello A, Jung Y, Yang L, Popov Y, Choi SS, Witek RP, Alpini G, Venter J, Vandongen HM, Syn WK, Baroni GS, Benedetti A, Schuppan D, Diehl AM.** Hedgehog signaling regulates

epithelial-mesenchymal transition during biliary fibrosis in rodents and humans. *J Clin Invest* 118: 3331–3342, 2008.
26. **Pardo A, Barrios R, Gaxiola M, Segura-Valdez L, Carrillo G, Estrada A, Mejía M, Selman M.** Increase of lung neutrophils in hypersensitivity pneumonitis is associated with lung fibrosis. *Am J Respir Crit Care Med* 161: 1698–1704, 2000.
27. **Phan SH.** Biology of fibroblasts and myofibroblasts. *Proc Am Thorac Soc* 5: 334–337, 2008.
28. **Phanish MK, Wahab NA, Colville-Nash P, Hendry BM, Dockrell ME.** The differential role of Smad2 and Smad3 in the regulation of pro-fibrotic TGFbeta1 responses in human proximal-tubule epithelial cells. *Biochem J* 393: 601–607, 2006.
29. **Ramos C, Montaño M, Becerril C, Cisneros-Lira J, Barrera L, Ruíz V, Pardo A, Selman M.** Acidic fibroblast growth factor decreases alpha-smooth muscle actin expression and induces apoptosis in human normal lung fibroblasts. *Am J Physiol Lung Cell Mol Physiol* 291: L871–L879, 2006.
30. **Robinson CJ, Harmer NJ, Goodger SJ, Blundell TL, Gallagher JT.** Cooperative dimerization of fibroblast growth factor 1 (FGF1) upon a single heparin saccharide may drive the formation of 2:2:1 FGF1. FGFR2c heparin ternary complexes. *J Biol Chem* 280: 42274–42282, 2005.
31. **Selman M, King TE, Pardo A.** Idiopathic pulmonary fibrosis: prevailing and evolving hypotheses about its pathogenesis and implications for therapy. *Ann Intern Med* 134: 136–151, 2001.
32. **Selman M, Pardo A.** Role of epithelial cells in idiopathic pulmonary fibrosis. From innocent targets to serial killers. *Proc Am Thorac Soc* 3: 364–372, 2006.
33. **Selman M, Carrillo G, Estrada A, Mejia M, Becerril C, Cisneros J, Gaxiola M, Pérez-Padilla R, Navarro C, Richards T, Dauber J, King TE Jr, Pardo A, Kaminski N.** Accelerated variant of idiopathic pulmonary fibrosis: clinical behavior and gene expression pattern. *PLoS ONE* 2: e482, 2007.
34. **Selman M, Pardo A, Kaminski N.** Idiopathic pulmonary fibrosis: aberrant recapitulation of developmental programs? *PLoS Med* 5: e62, 2008.
35. **Shukla MN, Rose JL, Ray R, Lathrop KL, Ray A, Ray P.** Hepatocyte growth factor inhibits epithelial to myofibroblast transition in lung cells via Smad7. *Am J Respir Cell Mol Biol* 40: 643–653, 2009.
36. **Taki M, Verschueren K, Yokoyama K, Nagayama M, Kamata N.** Involvement of Ets-1 transcription factor in inducing matrix metalloproteinase-2 expression by epithelial-mesenchymal transition in human squamous carcinoma cells. *Int J Oncol* 28: 487–449, 2006.
37. **Tian YC, Chen YC, Chang CT, Hung CC, Wu MS, Phillips A, Yang CW.** Epidermal growth factor and transforming growth factor-beta1 enhance HK-2 cell migration through a synergistic increase of matrix metalloproteinase and sustained activation of ERK signaling pathway. *Exp Cell Res* 313: 2367–2377, 2007.
38. **Trimboli AJ, Fukino K, de Bruin A, Wei G, Shen L, Tanner SM, Creasap N, Rosol TJ, Robinson ML, Eng C, Ostrowski MC, Leone G.** Direct evidence for epithelial-mesenchymal transitions in breast cancer. *Cancer Res* 68: 937–945, 2008.
39. **Valcourt U, Kowanetz M, Niimi H, Heldin CH, Moustakas A.** TGF-β and the Smad signaling pathway support transcriptomic reprogramming during epithelial-mesenchymal cell transition. *Mol Biol Cell* 16: 1987–2002, 2005.
40. **Wells A, Yates C, Shepard CR.** E-cadherin as an indicator of mesenchymal to epithelial reverting transitions during the metastatic seeding of disseminated carcinomas. *Clin Exp Metastasis* 25: 621–628, 2008.
41. **Willis BC, Liebler JM, Luby-Phelps K, Nicholson AG, Crandall ED, du Bois RM, Borok Z.** Induction of epithelial-mesenchymal transition in alveolar epithelial-like cells by transforming growth factor-beta1: potential role in idiopathic pulmonary fibrosis. *Am J Pathol* 166: 1321–1332, 2005.
42. **Xu J, Lamouille S, Derynck R.** TGF-beta-induced epithelial to mesenchymal transition. *Cell Res* 19: 156–172, 2009.
43. **Yang YC, Piek E, Zavadil J, Liang D, Xie D, Heyer J, Pavlidis P, Kucherlapati R, Roberts AB, Bottinger EP.** Hierarchical model of gene regulation by transforming growth factor beta. *Proc Natl Acad Sci USA* 100: 10269–10274, 2003.
44. **Yao HW, Xie QM, Chen JQ, Deng YM, Tang HF.** TGF-beta1 induces alveolar epithelial to mesenchymal transition in vitro. *Life Sci* 76: 29–37, 2004.
45. **Yilmaz M, Christofori G.** EMT, the cytoskeleton, and cancer cell invasion. *Cancer Metastasis Rev* 28: 15–33, 2009.
46. **Zakrzewska M, Wiedlocha A, Szlachcic A, Krowarsch D, Otlewski J, Olsnes S.** Increased protein stability of FGF1 can compensate for its reduced affinity for heparin. *J Biol Chem* 284: 25388–25403, 2009.
47. **Zeisberg M, Shah AA, Kalluri R.** Bone morphogenic protein-7 induces mesenchymal to epithelial transition in adult renal fibroblasts and facilitates regeneration of injured kidney. *J Biol Chem* 280: 8094–8100, 2005.
48. **Zhang F, Zhang Z, Lin X, Beenken A, Eliseenkova AV, Mohammadi M, Linhardt RJ.** Compositional analysis of heparin/heparan sulfate interacting with fibroblast growth factor.fibroblast growth factor receptor complexes. *Biochemistry* 48: 8379–8386, 2009.